International Journal of Biological Macromolecules 51 (2012) 1127–1133

International Journal of Biological Macromolecules

journal homepage: www.elsevier.com/locate/ijbiomac

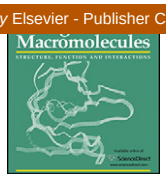

Chitosan/TPP microparticles obtained by microemulsion method applied in controlled release of heparin

Alessandro F. Martins*, Daiane M. de Oliveira, Antonio G.B. Pereira, Adley F. Rubira, Edvani C. Muniz

Grupo de Materiais Poliméricos e Compósitos, GMPC - Departamento de Química, Universidade Estadual de Maringá UEM – Av. Colombo 5790 – CEP 87020-900 Maringá, Paraná, Brazil

ARTICLE INFO

Article history:
Received 18 June 2012
Received in revised form 4 August 2012
Accepted 28 August 2012
Available online 2 September 2012

Keywords:
Chitosan
Heparin
Controlled release
Tripolyphosphate
Microparticles

ABSTRACT

This work deals with the preparation of chitosan/tripolyphosphate microparticles (CHT/TPP) using microemulsion system based on water/benzyl alcohol. The morphology of the microparticles was evaluated by scanning electron microscopy (SEM). The microparticles were also characterized through infrared spectroscopy (FTIR) and wide-angle X-ray scattering (WAXS). The morphology and crystallinity of microparticles depended mainly on CHT/TPP ratio. Studies of controlled release of HP were evaluated in distilled water and in simulated gastric fluid. Besides, the profile of HP releasing could be tailored by tuning the CHT/TPP molar ratio. Finally, these prospective results allow the particles to be employed as site-specific HP controlled release system.

1. Introduction

Chitosan (CHT) is a non-toxic polymer obtained from deacetylation of chitin [1,2]. This polymer presents excellent biocompatibility, biodegradability and antimicrobial activity [3]. Thus, CHT has been studied for many medical applications such as tissue engineering and drug delivery systems [1–6]. As the CHT possesses higher adsorption capacity than chitin, therefore, the CHT-based materials could be utilized in water purification systems [7]. The TPP is a non-toxic polyanion which interacts with CHT through electrostatic forces. The protonated amine groups in CHT interact with the negatively charged ions on TPP through ionic interactions creating ionic cross-linked networks [8–10]. Microparticles of CHT crosslinked with tripolyphosphate (TPP) showed significant results in adsorption of ions Copper(II) [8], Lead(II) [9] and Uranium [10].

In the intestinal environment, CHT/TPP particles showed potential for specific delivering of Papain [11], Acyclovir (antiviral drug) [12] and polyphenolic antioxidants, such as Catechin [13]. Chitosan/cyclodextrin nanoparticles were also used as devices for controlled release of heparin (HP) [14]. The low encapsulation efficiency and high association of the drug with chitosan/cyclodextrin nanoparticles impaired the release of HP [14]. Chitosan/genipin microspheres showed potential for specific delivering of low molecular weight heparin (LMWHP) in the region of the gastrointestinal tract [15]. However, it is known that LMWHP does not present effective anticoagulant activity [16].

The molecule of HP consists of sulfated D-glucosamine units, joined in alternating sequence by α(1,4)-glycosidic linkages, to either D-glucuronic and L-iduronic acid [17–19]. Due to the presence of carboxyl and sulfate groups, HP has the highest negative charge density of any known biological polyanion [19]. The HP presents interesting properties such as biodegradability, biocompatibility, stimulates cell growth and inhibits blood coagulation, so it is widely used in pharmaceutical and medical fields [3,17,18].

The aims of this study were to obtain CHT/TPP particles through microemulsion method at different pH and CHT/TPP ratios, using the system water/benzyl alcohol, to encapsulate the HP on such particles and to evaluate the profiles of HP release at different pH conditions.

2. Experimental

2.1. Materials

Chitosan (CAS 9012-76-4) with deacetylation degree equal to 85% and average molecular weight of 87×10^3 g mol^{-1} was purchased from Golden-Shell Biochemical (China); benzyl alcohol (CAS 100-51-6) and methylene blue (CAS 97130-83-1) were both purchased from Sigma; sodium tripolyphosphate (85%) (CAS 9010-08-6) was purchased from Acros (New Jersey, USA). Heparin sodium (CAS 9041-08-1) was kindly supplied by Kin Master (Passo Fundo, Brazil). Other reactants such as, sodium hydroxide, sodium

* Corresponding author. Tel.: +55 44 3011 3676; fax: +55 44 3011 4125.
E-mail address: afmartins50@yahoo.com.br (A.F. Martins).

0141-8130
http://dx.doi.org/10.1016/j.ijbiomac.2012.08.032

Table 1
Composition of the microemulsion system (W/BnOH): the volumes of each solution, CHT/TPP molar ratio and pHs used to obtain of the particles.

	CHT/TPP molar ratio			
	15/1 (pH 2)	9/1 (pH 2)	15/1 (pH 5)	9/1 (pH 5)
CHT (cm^{-3})	20	20	20	20
TPP (cm^{-3})	3	5	3	5

chloride, hydrochloric acid, ethanol and acetone were also utilized in this work. All reactants were used as received, thus without further purification.

2.2. Particles preparation

Particles of CHT/TPP were prepared based on a microemulsion system using water/benzyl alcohol (W/BnOH) [20]. For preparing the CHT/TPP particles, separated solutions (20 cm^{-3}) of CHT (0.4 g or 2.48 mmol per repeating unit, being considered only the deacetylated residues) and TPP (0.47 g or 1.09 mmol) at 2.0 wt.%/vol.% were prepared at pH 2 and pH 5. The pH was adjusted by either sodium hydroxide or hydrochloric acid (1.0 or 0.10 mol L^{-1}) solutions. The previously prepared solution of CHT (20 cm^{-3}) was mixed with benzyl alcohol keeping the volume ratio at 1/4 (W/BnOH). The mixture was initially kept under stirring at 6000 rpm during 10 min and then increased to 14,000 rpm. Afterwards, 3.0 or 5.0 cm^{-3} (TPP solution) was slowly dripped and the system was kept under stirring by further 10 min. Finally, the particles of CHT/TPP were precipitated and washed in acetone, vacuum filtered and dried at 30 °C for 24 h. The volume of each solution and CHT/TPP molar ratios, as well as the pH in which the particles were prepared are summarized in Table 1. The label CHT/TPP*x*–*y* was used for correlating the pH(*x*) and volume (*y*) of TPP solution, used for preparing the particles, to the studied properties.

2.3. Particles characterization

2.3.1. Scanning electron microscopy (SEM)

The morphology of particles was investigated through analysis of SEM images (Shimadzu, model SS 550). The particles were sputter-coated with a thin layer of gold for allowing the SEM visualization. Images were taken by applying an electron beam accelerating voltage of 10–15 kV. The particles average diameters were calculated by analysis of SEM images using the software Size Meter©, version 1.1 with differentiation threshold set according to the image scale.

2.3.2. Wide angle X-ray scattering (WAXS)

The WAXS profiles were recorded on a diffractometer Shimadzu model XRD-600 equipped with a Ni-filtered Cu-K_α radiation. The WAXS profiles were collected in the scattering range $2\theta = 5–70°$, with resolution of 0.02°, at a scanning speed of 2° min^{-1}. The analyses were performed by applying an accelerating voltage of 40 kV and a current intensity of 30 mA.

2.3.3. Fourier-transform infrared spectroscopy (FTIR)

FTIR spectra were recorded using a Fourier transform infrared spectrophotometer (Shimadzu Scientific Instruments, Model 8300, Japan), operating from 4000 to 500 cm^{-1}, at resolution of 4 cm^{-1}. FTIR spectra were obtained from KBr pellets. For comparison, the raw CHT and HP were also characterized by the FTIR technique.

2.4. Loading of HP on CHT/TPP particles

1.0 g of each sample (CHT/TPP*x*–*y* particles) was dispersed in ca. 90 cm^3 of HCl/H_2O solution at (pH 2 or pH 5) under stirring at 1000 rpm. Just after, 10 cm^3 of HP solution (1.0 mg cm^{-3}) was slowly dripped. The system was kept under stirring (1000 rpm) over 24 h at room temperature. So, the loaded particles were removed by centrifugation (14,000 rpm) at 4 °C, vacuum filtered, washed with ethanol and lyophilized for 24 h at −55 °C. The supernatant was analyzed through UV spectroscopy technique (at $\lambda = 567$ nm using a UV-Vis Femto, model 800Xi, Brazil) to estimate the loading efficiency. Aliquots of 100 μL of supernatant were directly added to 4.0 cm^3 of an aqueous solution of methylene blue (MB) (5.0 mg L^{-1}), according to methodology described by Farndale et al. [21] and Martins et al. [3]. The measurements of absorbance of the complex MB/HP were performed immediately after homogenization of the samples that occurred quickly after mixing. Using a previously built analytical curve, the concentration of HP remained in the supernatant was calculated [3]. The analytical curve was designed from standard HP solutions varying from 0.20 to 7.0 mg L^{-1} using distilled water as solvent (pH ≈ 5.5–6.0). Such analytical curve was made based on increasing absorbance of the complex of MB/HP with increasing concentration of HP. The value of linear correlation coefficient (R^2) for such curve was 0.987. The encapsulation efficiency was calculated using the following equation:

$$\text{Encapsulation efficiency} = \frac{[HPi] - [HPs]}{[HPi]} \times 100\% \quad (1)$$

where [*HPi*] is initial amount of heparin and [*HPs*] is the amount of heparin in the supernatant.

2.5. Characterization of the loaded particles

2.5.1. FTIR spectroscopy

The HP-loaded CHT–TPP particles were also characterized by FTIR spectroscopy in the same way as already described for non-loaded particles.

2.5.2. Thermogravimetric (TGA/DTG) analysis

TGA was performed from 25 °C to 750 °C at a heating rate of 10 °C min^{-1} under $N_{2(g)}$ flowing at 50 mL min^{-1} in a TGA-50 Thermogravimetry Analyzer (Netzch, model STA 409PG/4/G Luxx, USA).

2.6. In vitro heparin (HP) release

The in vitro HP release studies were performed in two different environments: simulated gastric fluid (SGF, 2.0 g NaCl and 7.0 cm^{-3} HCl in 1000 cm^{-3} of water, pH 1.2) and distilled water (pH ≈ 5.5–6.0), both without the presence of enzymes. In a dissolutor apparatus, 0.20 g of loaded particles were deposited in a sealed flask with 50 cm^{-3} of SGF or distilled water under constant stirring (60 rpm), at 37 °C. At a desired time interval, an aliquot (100 μL) was removed from the flask and directly added to 4.0 cm^3 of aqueous MB solution (5.0 mg L^{-1}), to quantify the released amount of drug through UV measures, as described in Section 2.4. In this case, analytical curve for HP solution at SGF and at distilled water were built in the HP conc. range of 0.20–7.0 mg L^{-1} [3,21]. The linear correlation coefficient (R^2) for the analytical curve using the SGF as solvent was of 0.986. The fraction released of HP was calculated from the following equation:

$$\text{Fraction released} = \frac{\text{amount released}}{\text{amount encapsulated}} \times 100\% \quad (2)$$

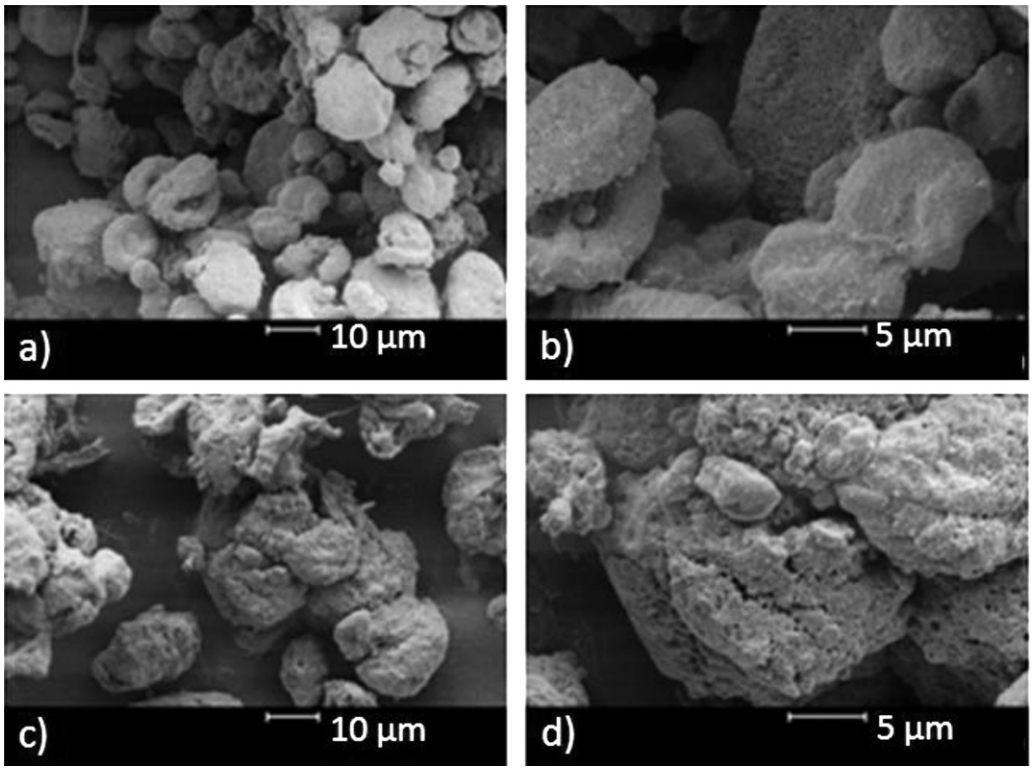

Fig. 1. SEM images of the CHT/TPP2–3 (a and b) and CHT/TPP2–5 (c and d) particles.

3. Results and discussion

3.1. Particles characterization

3.1.1. Scanning electron microscopy (SEM)

SEM images in Figs. 1 and 2 allow observing that the morphology of obtained particles is dependent on CHT/TPP molar ratio and on pH of feed solution. The lower CHT/TPP ratio at pH 2 (see Table 1) did not favor the formation of small particles due to coalescence but favors, in fact, irregularly shaped large clusters, as showed in Fig. 1c and d. Therefore, those samples were not used for further studies in this work. The values of averaged particles size obtained after different runs are presented in Table 2.

The samples obtained from feed solution at pH 5, CHT/TPP5–3 and CHT/TPP5–5, did not coalesce as those prepared at pH 2 (compare the Figs. 1 and 2). However, it could be verified that the lower CHT/TPP molar ratio (at pH 5) favors the formation of more compacted particles; see Fig. 2a–c. Therefore, the CHT/TPP ratio and the pH clearly influenced the size and porosity of obtained particles. In general, the CHT/TPP particles presented irregular shape.

3.1.2. WAXS profiles

Fig. 3 shows the WAXS profiles of CHT and of CHT/TPP particles at three different formulations. One could observe the CHT/TPP particles showed important differences in the crystallinity profile as compared to pure CHT. The diffraction peaks that appear in WAXS profile of CHT (Fig. 3a) at $2\theta = 10.5^\circ$, 19.9°, 43.9° and 64.3° were attributed to the crystalline regions formed by hydrogen bonds among the amino and hydroxyl groups on CHT chains [17,22]. It is possible to verify on profiles presented in Fig. 3 that the CHT/TPP2–3 and CHT/TPP5–3 particles presented higher crystallinity than the CHT/TPP5–5 ones, fact directly associated to CHT/TPP molar ratio. The lower crosslinking density (related to the used amount of TPP) the higher is the CHT chains mobility, feature that contributes to the reorganization of CHT chains during the formation of CHT/TPP2–3 and CHT/TPP5–3 particles.

Table 2
Average size of CHT/TPP particles.

Particles	Particles size (μm)	
	3 cm^{-3} (TPP)	5 cm^{-3} (TPP)
CHT/TPP2	9.23 ± 3.8	–
CHT/TPP5	7.26 ± 2.3	10.56 ± 4.2

The CHT chains reorganization is evidenced by the intense peaks that appear at $2\theta = 12.2^\circ$, 44.0° and 64.5° (Fig. 3, curves b and c on). Piai et al. [22] and Fajardo et al. [23] observed reorganization in polyelectrolyte complexes (PECs) constituted by CHT and chondroitin sulfate by analyzing the diffraction peaks at $2\theta = 43.8^\circ$ and 64.2° in WAXS profile of such PECs. The high intensity of such new peaks in Fig. 3, related to WAXS profile of raw CHT (curve a), was attributed to the large extension of H-bonds among CHT–CHT, CHT–TPP and TPP–TPP chain segments. Unlike the amino groups of CHT, which possessed $pK_a \approx 6.5$, the TPP anion presents five pK_a ($pK_{a1} = 1.0$, $pK_{a2} = 2.0$, $pK_{a3} = 2.79$, $pK_{a4} = 6.47$ and $pK_{a5} = 9.24$), according to Shu and Zhu [24]. So, the TPP anion can contribute to the increase the intermolecular forces in the CHT/TPP particles, since not all of phosphate groups are ionized in acid medium [24].

Fig. 4 depicts the proposed scheme for the aforementioned interactions. In light of this, the reorganization of CHT chains is favored when the used amount of TPP is not enough to neutralize the density of positive charges on CHT, that prevail as $^+NH_3$.

Besides, the large extent of positive charges due to the high CHT/TPP molar ratio on CHT/TPP2–3 and CHT/TPP5–3 particles could induce the appearance of domains with electrostatic repulsion (Fig. 4). These repulsion sites could be minimized with structural reorganization process increasing the density of interactions through H-bonds on CHT/TPP2–3 and CHT/TPP5–3 particles (Fig. 4). This fact would explain the higher crystallinity of those samples related to CHT/TPP5–5.

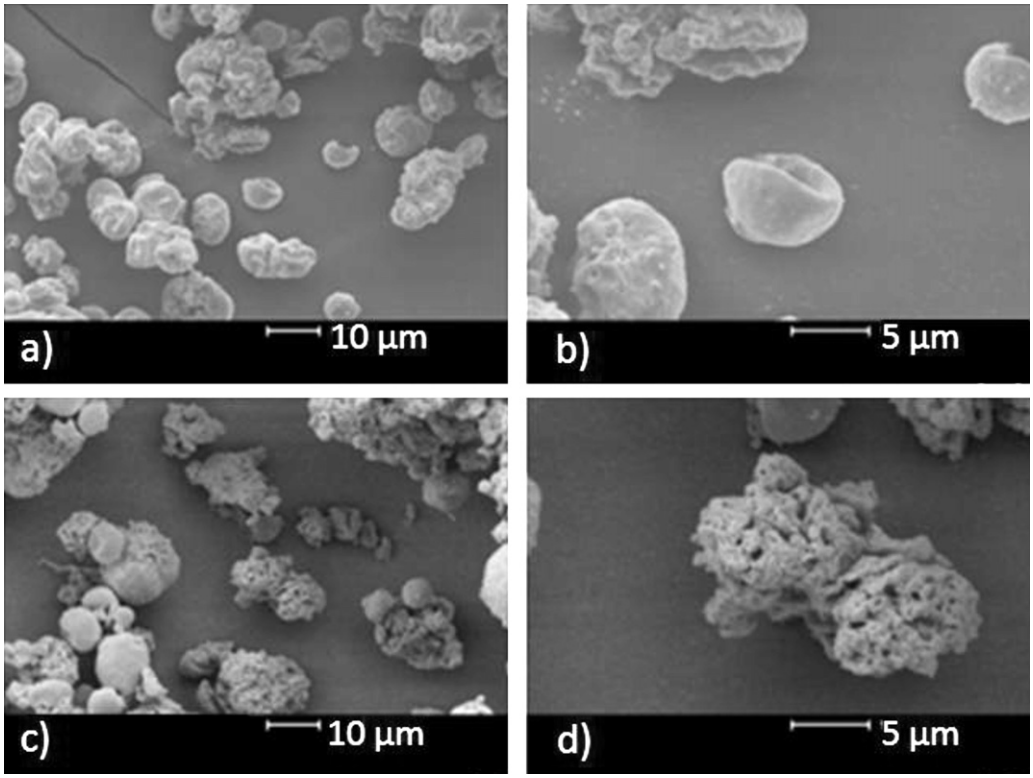

Fig. 2. SEM images of the CHT/TPP5–3 (a and b) and CHT/TPP5–5 (c and d) particles.

On the other hand, from the curve (d) on Fig. 3, it is possible to observe that CHT/TPP5–5 particles are mostly amorphous, fact proved by the occurrence of a halo with maximum at $2\theta = 21.8^\circ$ and also by the absence of peaks at $2\theta = 12.2^\circ$, 44.0° and 64.5°, as compared to the WAXS profiles (curves b and c). In this way, the higher amount of TPP used in preparation of CHT/TPP particles (Table 1) the higher is the density of physical crosslinking. This fact provides larger rigidity of the chains, which hinders the reorganization of CHT chains in CHT/TPP5–5 particles.

From the analysis of SEM image from CHT/TPP5–5 particles (Fig. 2d), one can be inferred that the higher content of TPP ($5.0\,cm^{-3}$) provides rigidity to the CHT chains preventing its structural reorganization and leading to particles with highly uneven shape. Therefore, the low crystallinity and high roughness of CHT/TPP5–5 sample, in relation to the others, was mainly due to its low CHT/TPP molar ratio.

Additionally, the structural reorganization observed in the WAXS profiles (curves b and c) was confirmed by the absences of the diffractions peaks at $2\theta = 44.0^\circ$ and 64.5° in WAXS profile of pure sodium tripolyphosphate (curve e).

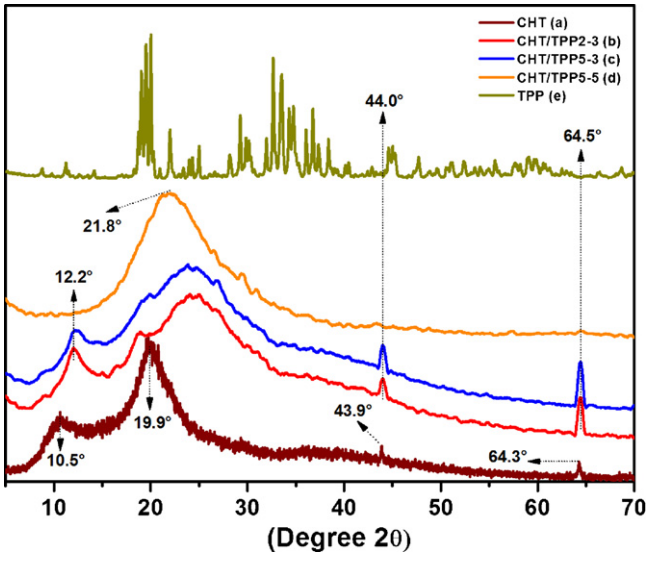

Fig. 3. WAXS profiles of precursors (CHT and TPP) and CHT/TPP particles.

3.1.3. FTIR spectroscopy

The CHT/TPP particles were characterized through FTIR spectroscopy, and the spectra are presented in Fig. 5. The FTIR spectrum of pure sodium tripolyphosphate (Fig. 5a) showed characteristic bands at 1218 (P—O stretching), 1156 (symmetrical and asymmetric stretching vibration of the PO_2 groups), 1094 (symmetric and asymmetric stretching vibration of the PO_3 groups) and 892 cm^{-1} (P—O—P asymmetric stretching) [25].

The main differences in the FTIR spectra of the particles related to FTIR spectrum of raw CHT, refers to the weak bands at 1250 cm^{-1} and 1218 cm^{-1} which can be assigned to P=O stretching vibration and the band at 892 cm^{-1} attributed to P—O—P asymmetric stretching (Fig. 5b–d). These signals indicate the presence of phosphate groups in the CHT/TPP particles [11,25,26]. The band at 1079 cm^{-1}, attributed to stretching of C—O bonds of primary alcohols (Fig. 5e), presented noticeable differences in comparison to the FTIR spectra of the particles (Fig. 5b–d). These differences were mainly due to complexation among CHT and TPP molecules [11]. The band at 1600 cm^{-1} that appears on CHT spectrum (Fig. 5e), attributed to N—H deformation of amine groups, is absent in the spectrum of CHT/TPP particles and a new band at 1523 cm^{-1}, assigned to $^{+}NH_3$, can be observed [11,26]. Therefore, from this spectral information, it can be concluded that the crosslinking was effective through ionic interactions among negatively charged P—O^{-} moieties of the phosphate groups of TPP and protonated $^{+}NH_3$ moieties of CHT chains. The, small differences in the FTIR spectra (range from

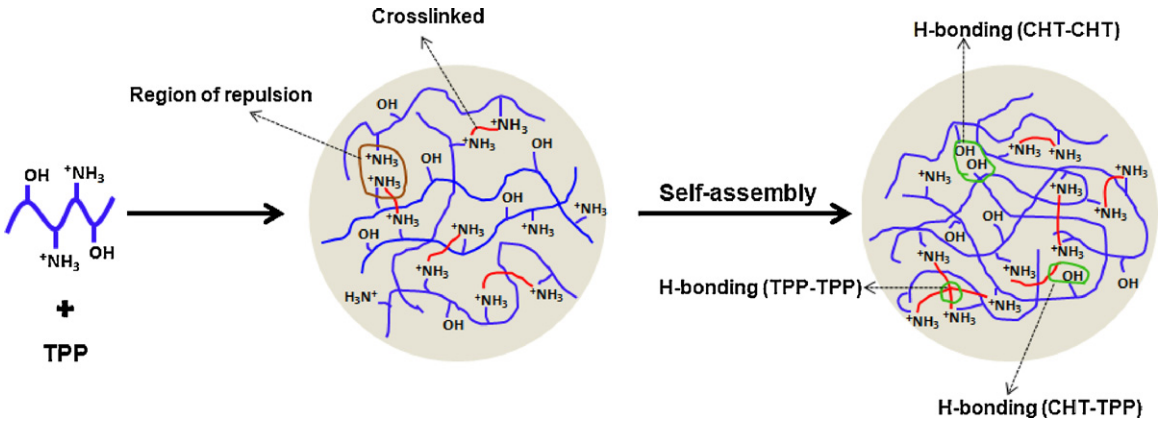

Fig. 4. Scheme depicting the physical crosslinking and self-assembly of CHT chains in CHT/TPP2–3 and CHT/TPP5–3 particles.

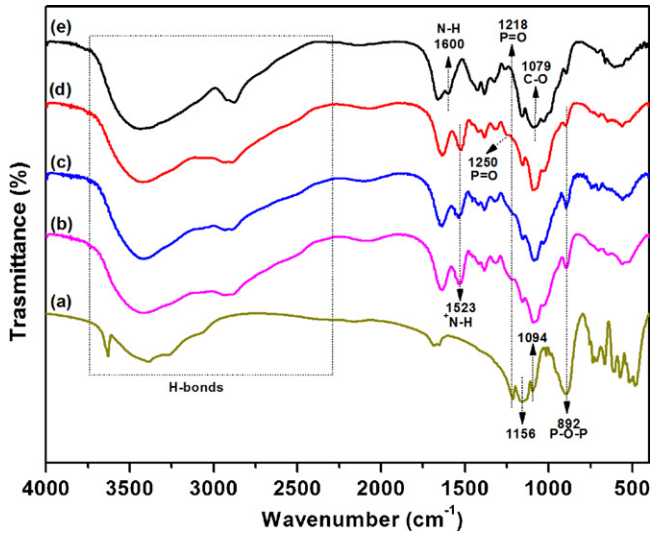

Fig. 5. FTIR spectrum of (a) TPP, (b–d) CHT/TPP particles and (e) CHT.

2250 to 3750 cm^{-1}) of the particles related to FTIR spectrum of CHT were assigned to the diversities in the H-bonds intensities among CHT–TPP and TPP–TPP chain segments. However, these spectral differences were subtle, since the H-bonds between the amino and hydroxyl groups on the CHT chains also are extremely pronounced, as related in Section 3.1.1.

3.2. Particles loading

3.2.1. Efficiency

The efficiency of HP loading was ca. 99% for all samples (Table 3) no important is the pH of solution used for loading neither the CHT/TPP ratio used during the particles preparation. This means that the natively charged HP would interact with remaining positive sites on CHT/TPP particles. The efficiency of HP loading was obtained according to methodology described by Martins et al. [3].

Table 3
Heparin encapsulation efficiency for various particles compositions ($n = 2$).

Particles	Encapsulation efficiency (%)
CHT/TPP2–3	99.0 ± 0.21
CHT/TPP5–3	99.2 ± 0.19
CHT/TPP5–5	99.4 ± 0.15

3.2.2. FTIR spectroscopy of HP-loaded particles

The HP-loaded CHT/TPP particles (CHT/TPP2–3/HP, CHT/TPP5-3/HP and CHT/TPP5-5/HP) were characterized by FTIR, as presented in Fig. 6. It is possible to observe clear spectral changes due to the incorporation of HP comparing the FTIR spectra of loaded and unloaded CHT/TPP2–3 particles (spectra *i* and *a*, respectively, Fig. 6). Firstly, the enlargement of the band at 1238 cm^{-1} (Fig. 6i) was attributed to the axial deformation of S=O groups from the saccharide structure of HP (Fig. 6d) [3]. Besides, a broadening in the region from 2500 cm^{-1} to 3500 cm^{-1} can be also verified. It is worthy to mention that at pH 2, the CHT chains present high density of positive charges, which strongly contributes to ionic association with polyanions [3,27]. This set of information confirms the HP encapsulation and also suggests that at pH 2 there is stronger association among HP chains and CHT/TPP2–3 particles than at pH 5, probably due to existing H-bonds and electrostatic interactions among $^{+}NH_3$ and OSO_3^- groups. This explains, for instance, the high efficiency in loading the HP on CHT/TPP particles.

On the other hand, the FTIR spectra for the loaded and unloaded particles prepared at pH 5 did not show any important difference. The only variation to be mentioned is the increase in intensity of the band at 2934 cm^{-1} attributed to the C—H axial deformation on HP [3]. The bands at 1521 cm^{-1} and 1637 cm^{-1} showed some variations in intensity; however this fact was associated with the weight of particles in the KBr pellets. In light of this, it is suggested

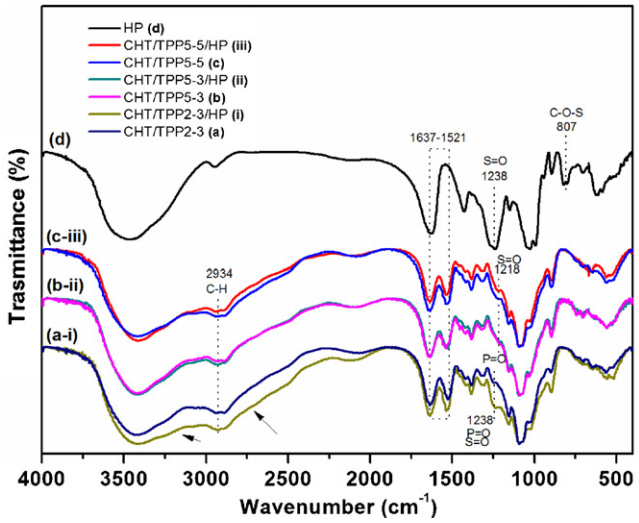

Fig. 6. FTIR spectra of CHT/TPP particles (a–c); CHT/TPP particles with loaded HP (i–iii); and HP (d).

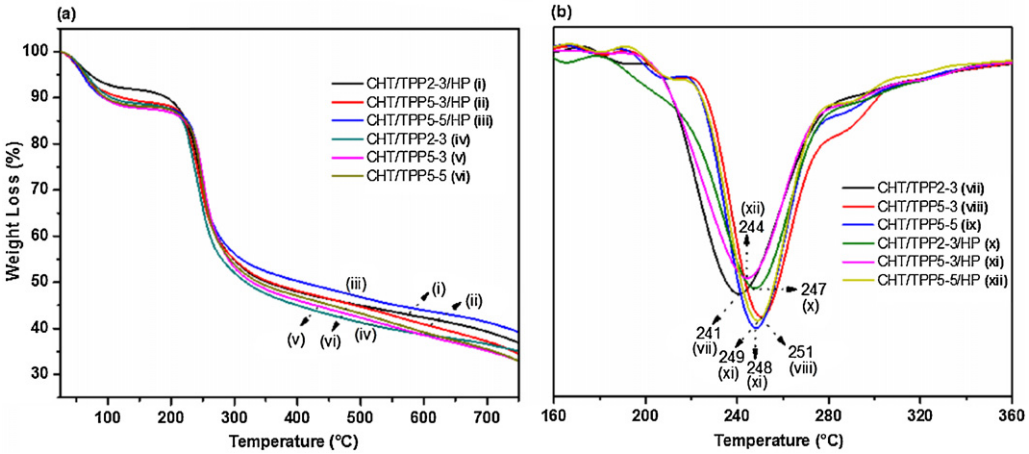

Fig. 7. TGA and DTG curves of the CHT/TPP and CHT/TPP particles with loaded HP.

that HP is mainly adsorbed in the surface of obtained particles. On other hand, the small differences in the FTIR spectra (Fig. 6) were mainly due to low weight proportion of HP on the loaded particles, when compared to the unloaded samples. For each 1.0 g of particle, only 9.9 mg of HP were loaded. Therefore, the small differences observed in the FTIR spectra (Fig. 6) were attributed to the HP-loading process.

3.2.3. Thermal stability of particles (TGA/DTG analysis)

The TGA curves from CHT/TPP and CHT/TPP/HP particles are presented Fig. 7a. It could be observed two thermal events of weight loss in each curve. The first one was attributed to the loss of water and also of volatile compounds. The CHT/TPP2–3, CHT/TPP5–3 and CHT/TPP5–5 particles presented similar amounts of adsorbed water, ca. 11 wt%. However, the samples CHT/TPP showed different water content than CHT/TPP/HP ones. The HP incorporation decreased the water content of the samples. This fact was stronger in the CHT/TPP2–3/HP and CHT/TPP5–3/HP samples. The sulphonate groups ($-OSO_3^-$) present in the HP structure strongly interact to $^+NH_3$ groups from CHT, decreasing the interaction (H-bond, dipole–dipole and ion–dipole) intensity among water molecules and CHT chains.

The TGA profiles from the CHT/TPP5–5 and CHT/TPP5–5/HP are very similar mainly if the first thermal event is taken into account. This information correlates to those from WAXS profiles (Fig. 3). The non reorganization of CHT chains in the CHT/TPP5–5 particles indicates that the polysaccharide segments are not enough available for interacting to water molecules as probably occurred in the other samples.

The first derivatives of degradation stage (second event on TGA curves) for CHT/TPP and CHT/TPP/HP are presented in Fig. 7b. It is possible to observe that samples presented different degradation temperatures, as indicated by the inflexion points in the DTG curves. This fact reinforces the HP encapsulation. The samples CHT/TPP2–3, CHT/TPP5–3 and CHT/TPP5–3 showed degradation temperatures of 241 °C, 251 °C and 248 °C, respectively. These differences were attributed mainly to the pH in which the particles were prepared. At low pH condition, the TPP did not stabilize the excess of $^+NH_3$ groups on CHT. So, there are domains in which the electrostatic repulsion (see Fig. 4) prevails, contributing to less packed structure, which provides to CHT/TPP2–3 lower thermal stability compared to the other two samples.

The adsorption of HP by the CHT/TPP2–3 particles raises the thermal stability in ca. 6 °C, from 241 °C to 247 °C. This fact was due to the further neutralization of remaining positive charges on CHT by HP that also provides extra H-bonds allowing increasing the thermal stability of CHT/TPP/HP2–3 sample.

On the other hand, the thermal stability of CHT/TPP5–3 decreased from 251 °C to 244 °C due to the encapsulation of HP (CHT/TPP5–3/HP). At pH 5, the presence of COO^- and OSO_3^- groups on HP allows repulsion on composite material leading to a smaller thermal stability compared to not HP-loaded particles. Finally, it

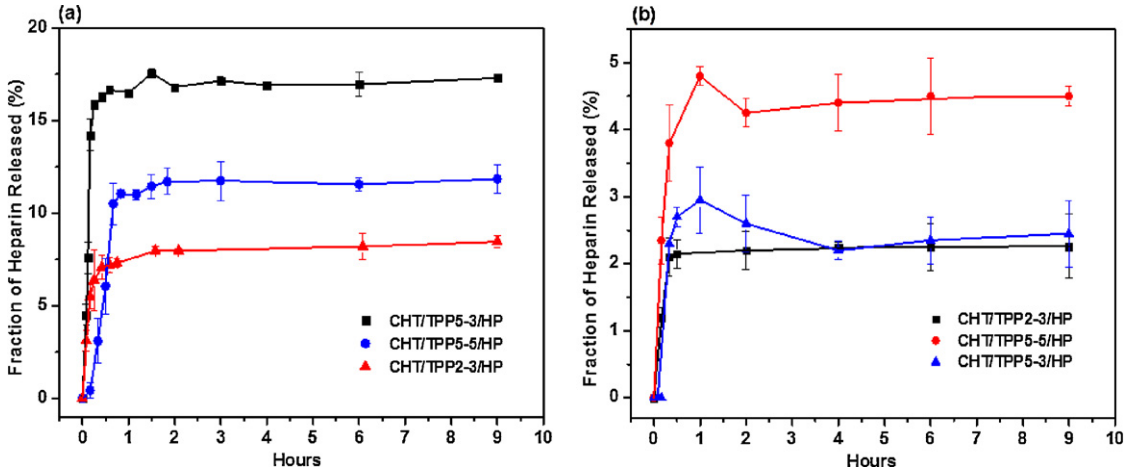

Fig. 8. Fraction of HP released from CHT/TPP particles in distilled water (a) and in SGF (b).

can be seen that the incorporation of HP on CHT/TPP5–5 particles practically did not affect the thermal stability of the sample (inflection point of TGA for CHT/TPP5–5 occurs at 248 °C and for CHT/TPP5–5/HP occurs at 249 °C).

As reported previously, for each 1.0 g of particle, only 9.9 mg of HP were loaded. Therefore, the weight ratio particle/HP is ca. 100/1 and TGA/DTG analyses were processed with only 6.0 mg of each sample (CHT/TPP loaded with HP and CHT/TPP unloaded). Thus, the small differences observed in Fig. 7 occur due to low weight of HP on the CHT/TPP loaded particles, when compared to the CHT/TPP unloaded samples. Thus, the subtle differences observed in the TGA/DTG curves also were assigned to the HP-loading process.

3.3. *"In vitro" release studies*

The fractions of HP released from CHT/TPP particles in distilled water and in SGF are presented in Fig. 8a and b, respectively. Considering the CHT/TPP5–3 particles, it was verified that the maximum fraction of HP released in distilled water was ca. 17% and it is achieved under 2 h (Fig. 8a) after the test has been initiated. This result shows that CHT/TPP5–3 particles present great potential to be used as device for sustained release of HP at neutral pH, and the almost same condition found in intestinal region.

The structure-loosing was due to the lower amount of TPP, the crosslinking agent used for preparing the CHT/TPP5–3 particles, and the pH close to 7 favored the HP releasing. An opposite characteristic was found for CHT/TPP2–3. This behavior can be understood by the higher association of the drug (HP) to the CHT/TPP particles obtained at pH 2, as previously discussed. The profile of HP released in SGF is presented in Fig. 8b. The particles presented stability in SGF and the extension of HP releasing was not as high as was observed in distilled water. Considering the CHT/TPP5–5 particles, the maximum releasing was 5% in SGF, for the first 1 h of analysis.

Following the same trend, CHT/TPP5–3 particles released only 2.5% of total loaded HP, while in distilled water the fraction of HP released was 17%. Therefore, the CHT/TPP microparticles could be successful used as site-specific drug delivery of HP in the intestinal region, especially the CHT/TPP5–3 particles.

4. Conclusions

CHT/TPP particles were successfully obtained from the microemulsion method (W/BnOH) at different CHT/TPP ratios and pH conditions. The particles were characterized by SEM, FTIR spectroscopy and WAXS. The morphology and crystallinity of particles depend mainly on CHT/TPP ratio. The HP encapsulation was ca. 99% for all tested samples as confirmed by TGA and FTIR techniques. Essays of controlled release of HP showed that CHT/TPP particles have high stability in SGF environment and in that condition the releasing of HP was minimized. On the other hand, in distilled water the CHT/TPP5–3 particles released ca. 17% (or 660 UI kg^{-1}) of the initially loaded HP. Therefore, CHT/TPP5–3 particles could act as a device for specific drug delivering of HP in the colon region. This study showed that the fraction of HP released could be tailored by tuning the amount of TPP used in the particles preparation. In light of this, lower CHT/TPP ratios could improve the extension of HP released from CHT/TPP particles at pH 5.

Acknowledgements

A.F.M. and A.G.B.P. thank, respectively, to CNPq (Brazil) and to CAPES (Brazil) for their doctorate fellowship. A.F.R. and E.C.M. thank to CNPq for the financial support.

References

[1] J.F. Piai, L.C. Lopes, A.R. Fajardo, A.F. Rubira, E.C. Muniz, Journal of Molecular Liquids 156 (2010) 28–32.
[2] S.H. Hua, H. Ma, X. Li, H. Yang, A. Wang, International Journal of Biological Macromolecules 46 (2010) 517–523.
[3] A.F. Martins, J.F. Piai, I.T.A. Schuquel, A.F. Rubira, E.C. Muniz, Colloid and Polymer Science 289 (2011) 1133–1144.
[4] H.T. Ta, H. Han, I. Larson, International Journal of Pharmaceutics 371 (2009) 134–141.
[5] K.H. Bae, C.W. Moon, Y. Lee, T.G. Park, Pharmaceutical Research 26 (2009) 93–100.
[6] V.K. Mourya, N.N. Inamdar, Journal of Materials Science Materials in Medicine 20 (2009) 1057–1079.
[7] A.J.M. Al-Karawi, Z.H.J. Al-Qaisi, H.I. Abdullah, Carbohydrate Polymers 83 (2011) 495–500.
[8] S.T. Lee, F.L. Mi, Y.J. Shen, Polymer 42 (2001) 1879–1892.
[9] L.F. Qi, Z.R. Xu, Colloids and Surfaces A 251 (2004) 183–190.
[10] M.K. Sureshkumar, D. Das, M.B. Mallia, Journal of Hazardous Materials 184 (2010) 65–72.
[11] F.C. Vasconcellos, G.A.S. Goulart, M.M. Beppu, Powder Technology 205 (2011) 65–70.
[12] H.K. Stulzer, M.P. Tagliari, A.L. Parize, M.A.S. Silva, M.C.M. Laranjeira, Materials Science & Engineering C-Biomimetic and Supramolecular Systems 29 (2009) 387–392.
[13] L. Zhang, S.L. Kosaraju, European Polymer Journal 43 (2007) 2956–2966.
[14] A.H. Krauland, M.J. Alonso, International Journal of Pharmaceutics 340 (2007) 134–142.
[15] R.H.E. Lecumberri, A. Heras, Marine Drugs 8 (2010) 1750–1762.
[16] G. Agnelli, Haemostasis 26 (1996) 2–9.
[17] A.F. Martins, A.G.B. Pereira, A.R. Fajardo, A.F. Rubira, M.C. Edvani, Carbohydrate Polymers 86 (2011) 1266–1272.
[18] D.K. Kweon, S.B. Song, Y.Y. Park, Biomaterials 24 (2003) 1595–1601.
[19] A.P. Zhu, Z. Ming, S. Jian, Applied Surface Science 241 (2005) 485–492.
[20] A.V. Reis, M.R. Guilherme, A.T. Paulino, E.C. Muniz, L.H.C. Mattoso, E.B. Tambourgi, Langmuir 25 (2009) 2473–2478.
[21] R.W. Farndale, D.J. Buttle, A.J. Barrett, Biochimica et Biophysica Acta 883 (1986) 173–177.
[22] J.F. Piai, A.F. Rubira, E.C. Muniz, Acta Biomaterialia 5 (2009) 2601–2609.
[23] A.R. Fajardo, J.F. Piai, A.F. Rubira, E.C. Muniz, Carbohydrate Polymers 80 (2010) 934–943.
[24] X.Z. Shu, K.J. Zhu, European Journal of Pharmaceutics and Biopharmaceutics 54 (2002) 235–243.
[25] F.-L. Mi, S.-S. Shyu, S.-T. Lee, T.-B. Wong, Journal of Polymer Science B 37 (1999) 1551–1564.
[26] Y. Luo, B. Zhang, W.H. Cheng, Q. Wang, Carbohydrate Polymers 82 (2010) 942–951.
[27] S. Boddohi, C.E. Killingsworth, M.J. Kipper, Biomacromolecules 9 (2008) 2021–2028.